P1.22 SEPARATING COMBUSTION FROM PYROLYSIS IN HIGRAD/FIRETEC

Jonah J. Colman* and Rodman R. Linn
Earth and Environmental Sciences Division
Los Alamos National Laboratory, Los Alamos, New Mexico

1. Abstract

HIGRAD/FIRETEC is a coupled atmosphere/wildfire behavior model based on conservation of mass, momentum, species and energy. It is a three-dimensional transport model that uses a compressible-gas formulation to couple its physics based wildfire model with the motions of the local atmosphere. In its current formulation combustion and pyrolysis are treated as a single process, which depends on the local densities of wood and oxygen, the levels of turbulent diffusion, and a probability distribution function (pdf) for temperature in the solid. The pdf is employed to give an 'ignited volume fraction', i.e. the fraction of wood within a resolved volume that is actively burning. This fuel model is now being extended to deal with pyrolysis and combustion as separate processes. Some fire behaviors, such as flash events, crowning, and fire 'whorls', may depend on the ability of combustion to take place in a separate spatial location from the pyrolysis. We refer to this fuel model as 'nonlocal'. In the nonlocal fuel model pyrolysis will be dealt with in roughly the same way as formerly, but it will now be an endothermic process. Instead of producing solely inert gasses, it will now produce a mixture of inert and combustible gasses. Combustion will now be dealt with as a separate process, which is highly exothermic. A separate pdf for the temperature in the gas phase will be defined. The basic premise of the HIGRAD/FIRETEC fuel model will be retained, i.e. that the rate of a reaction is limited by the rate at which the reactants can be brought together (mixing limited). In the nonlocal fuel model the reactants for pyrolysis can be thought of as heat and wood, for combustion the combustible gas and oxygen.

A few simple test cases utilizing idealized geometries will be simulated with both fuel models and the results compared.

* *Corresponding author address:*
Jonah J. Colman, Los Alamos National Laboratory, EES-2 MSD401, Los Alamos, NM, 87545; e-mail jonah@lanl.gov

2. Introduction

Wildfires are an extremely complex phenomenon involving feedbacks between fuel loads and moisture levels, local and regional topography, wind speeds and weather, and even combustion physics and small-scale turbulence. The science of predicting wildfire spread rates is not yet mature, but recent advances in computational resources have helped some progress be made. One of the major difficulties in constructing numerical models to study wildfire behavior is the enormous range of spatial scales that must be considered. A wildfire typically propagates on a km scale and geographical features on this scale are important to how they spread, local terrain and fuel characteristics can change on a scale of meters, fuel/oxygen mixing scales are on the order of mm, and combustion chemistry (such as gradients in radical species) operates on a sub μm scale. A similar analysis applies to temporal scales; a wildfire may burn for days while the combustion chemistry operates on sub μsec timescales. To run a useful physically based fire propagation simulation capturing the spatial scale of the wildfire as a whole is necessary. Under current computational constraints running a fluid dynamics simulation at this scale requires that the spatial resolution be near 1-100 m. Thus most of the combustion must be parameterized at as a subgrid phenomenon.

Current wildfire propagation models vary in origin from purely empirical formulations, (Andrews 1986; Finney 1998) to physics-based algorithms (Dupey and Larini 2000; Porterie *et al.* 2000; Grishin 2001A and 2001B) to combinations of the two (Clark *et al.* 1996 and 2004; Coen and Clark 2000). Models of differing complexity and origin are appropriate for different applications. FIRETEC (Linn 1997, Linn and Cinningham 2005) is a coupled atmospheric transport/wildfire

behavior model being developed at Los Alamos National Laboratory, and is based on the principals of conservation of mass, momentum, and energy as well as representations of some of the physical processes that drive wildfires. The physically based nature of FIRETEC could make it a useful learning tool and allow it to be used to examine some of the more complex wildfire behaviors. FIRETEC is combined with the hydrodynamics model, HIGRAD (Reisner *et al.* 2000 and 2003), in order to simulate wildfires using a terrain-following three-dimensional finite volume grid and a fully compressible gas transport formulation to couple its physics-based wildfire model with the motions of the local atmosphere. Some examples of the physical phenomena being studied with FIRETEC are the effects of transient wind conditions, nonhomogeneous terrain, nonuniform fuel beds with patchy distributions and different vertical fuel structures (Linn *et al.* 2002 and 2005). One unique feature of HIGRAD/FIRETEC is its self-determining nature. That is, no lookup table of fire propagation rates or other purely empirical formulations are used in its simulations.

In its current configuration HIGRAD/FIRETEC only models one reaction, which represents an idealized combination of pyrolysis and combustion. This reaction can only take place in the presence of solid fuel. While this formulation has had significant success, the present work examines the possibility of separating combustion from pyrolysis. That is modeling pyrolysis as an endothermic process in which combustible gasses are released, and then modeling the oxidation of the reactive portion of those gasses as a separate process. This would allow some transport of the reactive gas and for a flame to span more than one computational grid point. Typical average values for flame heights in grass fires range from 2-3 m for low wind speeds up to about 8 m for high wind speeds. HIGRAD/FIRETEC is typically run with a spatial resolution around 2 m. In extreme conditions whorls of superheated incompletely-combusted wood distillates can rise above wildfires and, reaching adequate oxygen supplies, ignite. Such structures can reach 50 to 100 m.

3. Model Formulation

Details as to the specific formulations of the HIGRAD or FIRETEC models or their numerical implementation are not related here but are available in other publications (Linn 1997, Linn *et al.* 2002, Linn and Cinningham 2005). In this work we are focused on the fuel model employed, and an extension of that work.

3.1 Local Fuel Model

The set of chemical reaction occurring in a wildfire is extremely complex and has many intermediate transient species. In the fuel model currently employed by firetec the set of chemical reaction was simplified to a single solid-gas reaction that is presented in equation 1.

$$N_{wood}(wood) + N_{O_2}(oxygen) \rightarrow (products) + (heat) \quad (1)$$

The stoichiometric coefficients, N_{wood} and N_{O2} describe the net amount of wood and oxygen consumed through pyrolysis and all of the intermediate reactions when a unit mass of 'inert' products is formed. The reaction rate (F_{wood}) is described by equation 2.

$$F_{wood} = \rho_{wood}\rho_{O_2}\sigma\Pi \quad (2)$$

Where ρ_{wood} and ρ_{O2} are the local densities of wood and oxygen respectively, σ is the turbulent diffusion coefficient, which is calculated based on the local turbulent kinetic energy and vegetation geometry, and Π is a function of: the stoichiometry assumed in equation (1), the local densities of the reactants, and a probability distribution function for the temperature (which is employed to give an 'ignited volume fraction', i.e. the fraction of wood in a resolved volume that is actively burning).

The philosophy behind this particular model is that the rate of pyrolysis is ultimately related to the heat flux to the solid wood, which is tied to the nearby gaseous reactions that are limited by the amount of oxygen. It is assumed that the rates of the exothermic reactions are limited by the rate at which reactants can be brought together (mixing limited), this is justified since the dominant exothermic reactions all involve oxidation by O_2, which is by far the limiting reagent in the case of actively burning wood. Thus, the heat fluxes to the solids, and so the rate of pyrolysis will ultimately be limited by the mixing

process. A simple function is used to represent the fraction of heat released from the gas phase that is deposited directly back to the solid, this function is assumed to be in direct proportion to the amount of wood that has burned. This is meant to represent the fact that the primary nature of burning at a given location changes over time from flaming combustion, with much of the heat escaping with the gases, to smoldering combustion where catalysis and insulation by char and ash cause a larger proportion of the heat to be recaptured by the solid.

3.2 Nonlocal Fuel Model

In the nonlocal fuel model we make the assumption that pyrolysis of wood creates inert and reactive gas species in an endothermic process. The reactive gas species are then allowed to combust in an exothermic process. It is assumed that some combustion is occurring on the surface of the burning particles, primarily non-volatile tars. Their heat of combustion is combined with that of pyrolysis. Pyrolysis is roughly 250 kJ/kg endothermic, and we estimate that the tar combustion is 50 kJ/kg exothermic. So we use 200 kJ/kg as the heat of pyrolysis. The rate of pyrolysis is dealt with using the local fuel model presented above with only minor adjustments. First, the limiting reagent for the pyrolysis is now heat rather than oxygen, oxygen is no longer consumed in the pyrolysis step. Second, the stoichiometry has changed.

$$\text{(wood)} \rightarrow N_{hc}\text{(reactive gas)} + N_{inert}\text{(inert gas)} - \text{(heat)} \quad (3)$$

$$N_{hc}\text{(reactive gas)} + N_{O_2}\text{(oxygen)} \rightarrow \text{(inert gas)} + \text{(heat)} \quad (4)$$

All the reactive gas species are lumped into one transportable gas. The stoichiometry was estimated with values taken from the experimental literature, specifically from estimates of the initial products from fast pyrolysis as shown in Table 1.

Table 1. Product composition from fast pyrolysis.

Product	Weight %[1]	Moles[2]	ΔH_{comb}(kJ/mol)	Total Heat (kJ)[4]	% ΔH_{wood}[5]
CO	46.9	202	-283	-57166	32
CH_4	6	45	-802.5	-36112.5	20.2
C_2H_4	3.5	15	-1323	-19845	11.1
C_2H_6	0.5	2	-1428.4	-2856.8	1.6
C_3H_6	1	3	-1802.1	-5406.3	3
H_2	2.5	149	-241.8	-36028.2	20.2
CH_3OH	4	15	-676.1	-10141.5	5.7
CH_3CHO	3.6	10	-1104.4	-11044	6.2
				-178600	
CO	16	44	0	0	0
H_2O	16	107	0	0	0

1. Weight percentages taken from *Hajaligol* [1982] and *Nunn* [1985].
2. Normalized integer values of mole fraction produced.
3. Heat of combustion for the specified product in kJ/mol.
4. Total energy produced by combustion of the number of moles specified in kJ. The value highlighted in yellow is the total energy produced.
5. The percentage contribution of the specified product to the total energy produced.

In terms of equation 3 this works out to: N_{hc} = 0.68 and N_{inert} = 0.32 . That is, 0.68 g of reactive gasses and 0.32 g of inert gasses are produced for each gram of wood pyrolyzed. Table 1 also converts the weight percentages into integer number of moles of each product. Then the total heat from the combustion of that number of moles of each product is then calculated assuming the final products are CO_2 and H_2O. In this way the stoichiometry and heat of combustion could be defined for the reactive gas.

$$C_{369}H_{882}O_{442} \rightarrow C_{325}H_{668}O_{227} + 44\,CO_2 + 107\,H_2O \quad (4)$$

Thus the reactive gas is represented $C_{325}H_{668}O_{227}$ and combusts according to the stoichiometry:

$$2\,C_{325}H_{668}O_{227} + 757\,O_2 \rightarrow 325\,CO_2 + 334\,H_2O \quad (5)$$

Represented in mass units this gives:

$$0.404\text{ g (reactive gas)} + 0.596\text{ g (oxygen)} \rightarrow 1\text{ g (inert gas)} \quad (6)$$

The heat of combustion is then: 178600 kJ/mole / 8208.74 g/mole = 21757.3 kJ/kg of reactive gas; or, 178600 kJ/mol / 20320.29 g/mol = 8789.24 kJ/kg of total reactants (reactive gas + oxygen). This compares with published estimates for solid fuel of 19378 kJ/kg and 8914 kJ/kg.

The reactive gas is then reacted with oxygen following a scheme proposed for FIRETEC by Linn (1997). The reaction rate (F_{gas}) is described by equation 7.

$$F_{\text{gas}} = \frac{\rho_{\text{reactivegas}}\rho_{O_2}\sigma\Pi}{2\left(N_{O_2}\rho_{reactivegas} + N_{\text{reactivegas}}\rho_{O_2}\right)} \quad (7)$$

Where the symbols have the same meaning as described for equation 2. There are some differences in the numerical constants used in the formulation of σ and Π. The new term in the denominator results from a simple description of the correlations between the density of the reactive gas and that of oxygen within a resolved volume. Once again this is a huge oversimplification of the complex chemistry occurring in gas phase combustion. It is simply meant as one step beyond the combustion chemistry currently employed by FIRETEC.

4. Simulations

All the simulations described in this work have three spatial dimensions and utilize a uniform horizontal grid resolution of 2 m with a 160-point domain in both directions (i.e. 320x320 m horizontal domain). The vertical grid spacing is non-uniform with a near ground resolution of approximately 1.5 m and increasing to about 30 m resolution at the top of the 41-point grid (615 m domain). Two different fuel distributions were considered. The first is meant to represent tall grass, which has an average height of 0.7 m, an average area distribution of 0.7 kg/m^2, and an initial moisture content of 5%. The second is meant as a crude representation of a stand of trees over dry grass. In this case the ground fuel is exactly the same as in the tall grass simulation, but most of the domain also has an overstory beginning at a height of 5 m and extending up to 10.6 m. The fuel in this overstory has an average area distribution of 0.2 kg/m^2 and an initial mosture content of 80%. For both fuel distributions the surface area per unit volume of the fuel is assumed to be 4000 m^{-1}. In all cases a neutral atmospheric stability is assumed.

Five simulations were run with the nonlocal fuel model. Equivalent runs were performed with the local fuel model for comparison purposes. Four tall grass simulations with different inlet wind speeds of: 1 m/sec, 3 m/sec, 6 m/sec, and 12 m/sec. These are referred to as runs u1, u3, u6, and u12 respectively. One forest simulation was also run with an inlet wind speed of 6 m/sec. The wind speeds are set as the boundary condition in what we describe as the x-direction. The wind quickly (a few seconds of simulated time) develops a shear profile due to the drag associated with the vegetation. The fires were ignited in a 100 m long, 4 m deep, area at grid points 55-105 in the y-direction and 30-31 in the x-direction. In these locations all fuel moisture was removed and the fuel temperature was raised from ambient (300 K) to 1000 K over a period of 2 seconds. In the forest runs the overstory began at location 41 in the x-direction and spanned the y-direction. Note that in the local fuel model simulations the fire was ignited in an equivalent fashion but that the locations were grid points 50-51 in the x-direction for the tall grass simulations.

4. Results

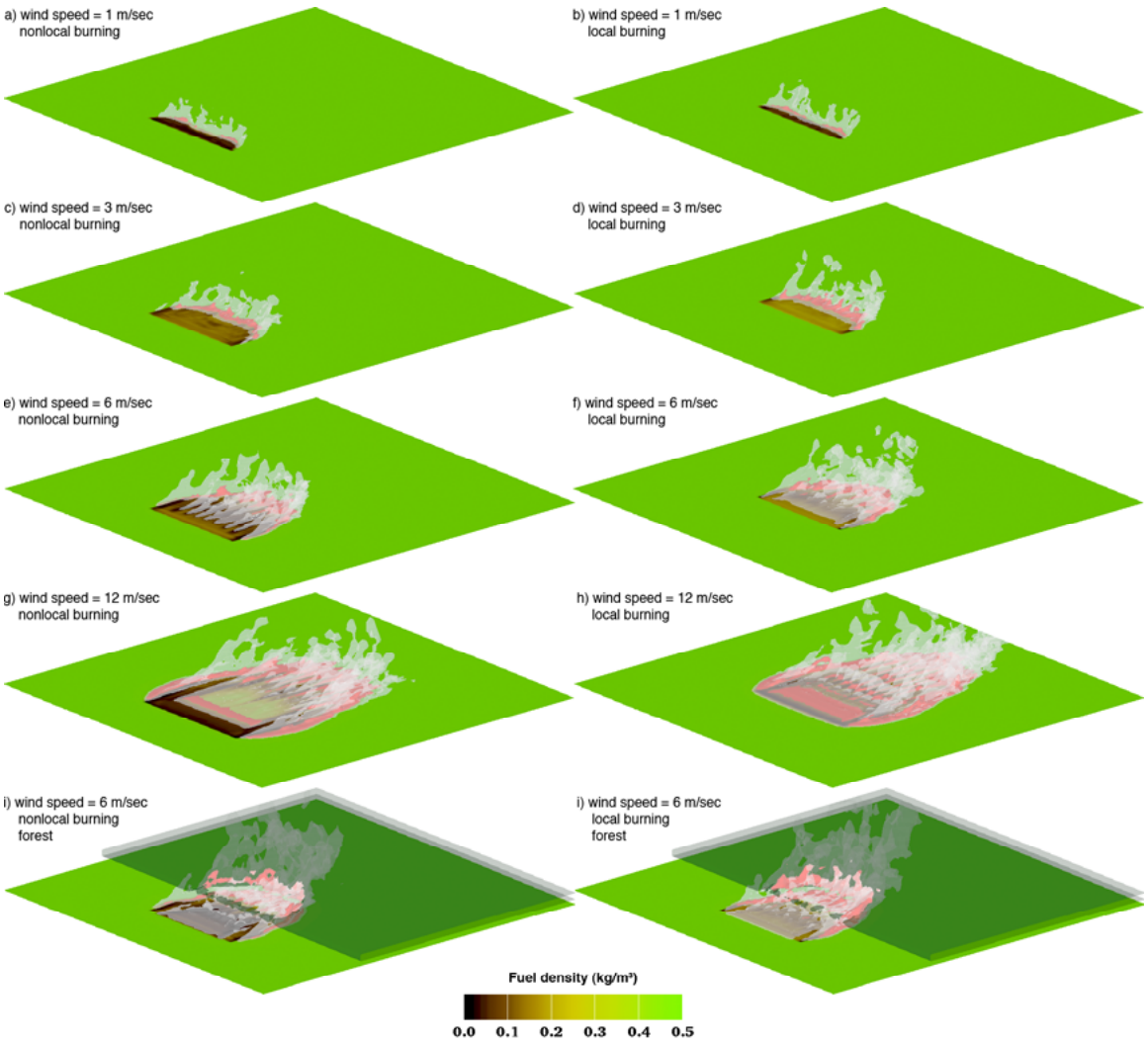

Figure 1. Isosurfaces of gas temperature in red (800 K), and transparent grey (400 K), after 60 seconds of simulated time. The horizontal surface depicts solid fuel density according to the color bar. In the forest simulations (i and j) there is an additional isosurface in transparent green that depicts locations where the overstory retains at least 75% of its initial density.

Figure 1 presents a visualization of each simulation with the nonlocal fuel model after 60 seconds of simulated time, beside a visualization of the corresponding local fuel model simulation. It is clear that each simulation responds to increasing inlet wind speeds with an increasing spread rate, and that the spread rates for the nonlocal fuel model are quite similar to those of the local model. To help quantify these basic trends a downwind spread distance is calculated as the farthest location downwind from the ignition line where the temperature of the solid fuel is raised above 500 K. The lateral spread distance can be similarly defined as the width (lateral to the inlet wind direction) of the region where the solid fuel temperature is above 500 K, minus the width of the initial ignition line. The lateral spread rate is then the time derivative of the lateral spread distance. The spread rates are then the time derivatives of the spread distances. Some care must be taken in calculating this rate as the method of ignition is somewhat arbitrary in the simulations, and boundary effects can also be important depending on the location of the fire. Figure 2 shows the spread distances plotted vs. time for all of the nonlocal tall grass simulations.

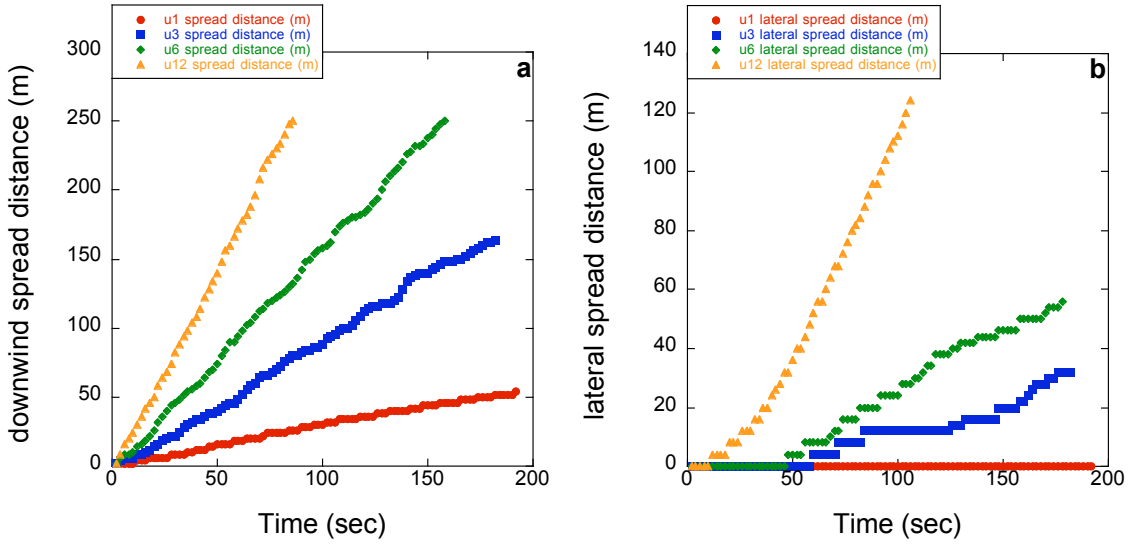

Figure 2. Spread distance in meters plotted vs. time in seconds for each of the tall grass simulations run with the nonlocal fuel model. Figure 2a shows the downwind spread distance plotted vs. time, and Figure 2b shows the lateral spread distance plotted vs. time.

In Table 2 the calculated downwind spread rates are presented for each simulation. In Figure 3 these spread rates are plotted along with values from the fire propagation model BEHAVE, which is based on the empirical equations described by Rothermel [1972], and values calculated from the empirical model described by Cheney [1998]. This comparison is useful as the empirical formulations were derived directly from data under conditions of relatively constant slope, winds, and homogeneous fuels. Comparisons with the Cheney values is straight forward as the wind speeds used as an input for this model are taken from standard anemometers at a height of 10 m off the ground, and the ambient wind obtained from the HIGRAD/FIRETEC model at this height is essentially equal to the inlet wind speed. Comparisons with BEHAVE are not as straightforward however. BEHAVE requires as input the ambient wind speed at the 'mid-flame height'. To help estimate what the equivalent values for our simulations is we ran HIGRAD/FIRETEC without a fire until the wind profile reached steady state. Considering the typical flame heights for grass fires and the available resolved heights in the simulation, wind speeds at a height of 2.26 m were chosen for the comparison with BEHAVE (the middle of our second vertical grid box). A good agreement is seen for both the local and nonlocal fuel models, though it should be noted that spread rate also depends on the size of the fire, specifically the length of the fireline.

Table 2. Spread rates calculated from HIGRAD/FIRETEC simulations.

Inlet Wind Speed (m/sec)	Wind Speed @ 2.28 m (m/sec)	Spread Rate, nonlocal fuel model (m/sec)	Spread Rate, local fuel model (m/sec)
1.0	0.72	0.24	0.27
3.0	1.9	0.91	0.79
6.0	4.2	1.64	1.37
12.0	7.7	3.12	3.22

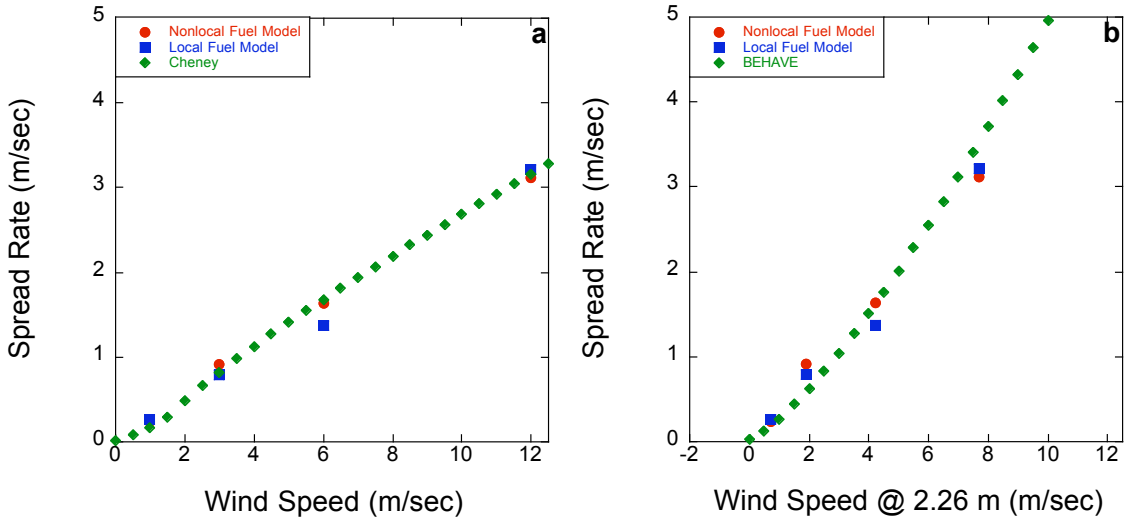

Figure 3. The spread rate in meters per second is plotted vs. the wind speed. In Figure 3a the inlet wind speed is used and results from the Cheney [1998] model are also plotted, in Figure 3b the wind speed at a height of 2.26 meters is used and results from the BEHAVE model are also plotted.

The lateral spread rate parameter is more difficult to compare and there are no reliable data to compare to, there are some reports of the overall fire perimeters shape and so we present fire perimeters for each of our simulations in Figure 4. Here locations where the initial solid fuel has been depleted by less than 10%, between 10% and 50%, and more than 50% are depicted in different colors.

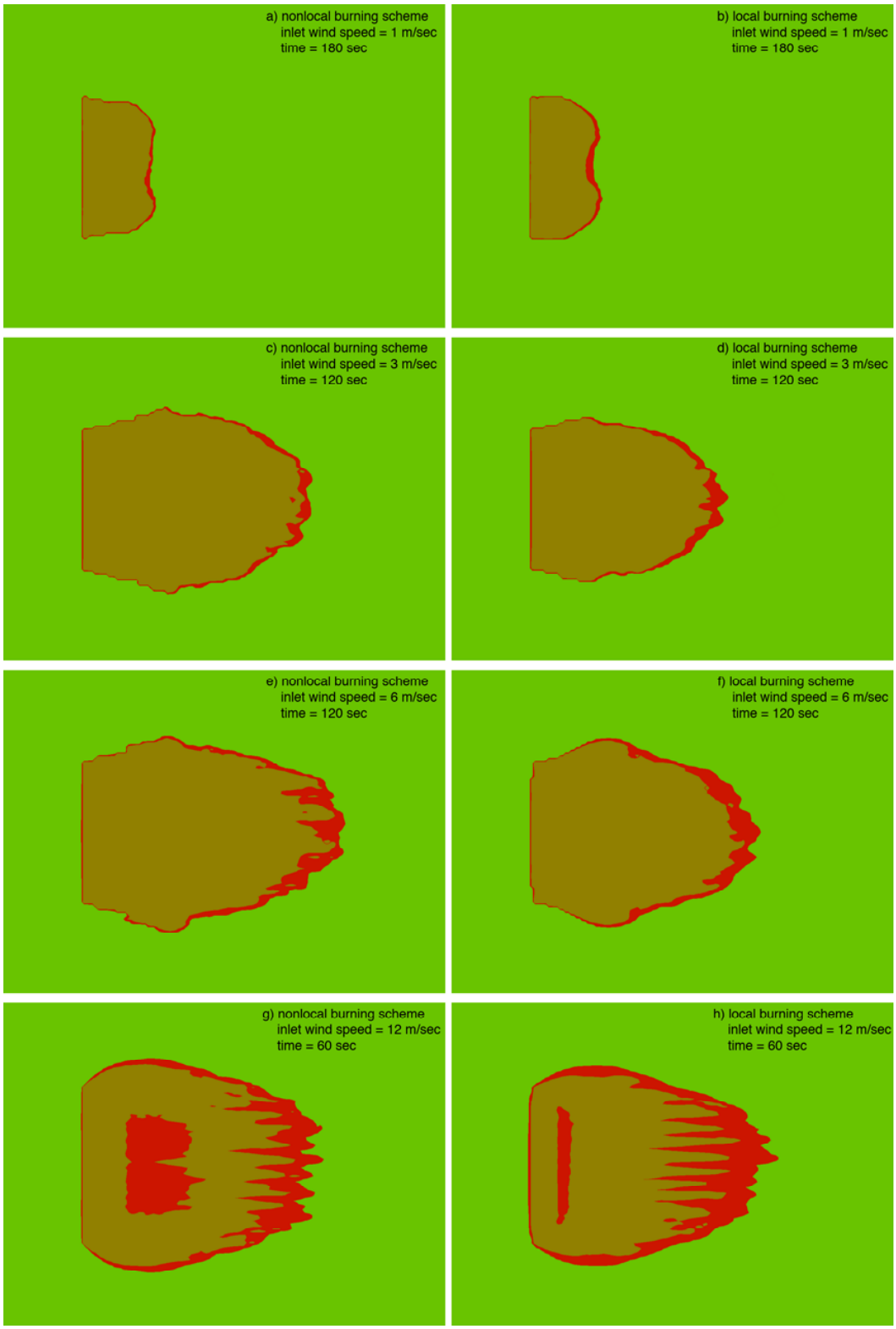

Figure 4. Fire perimeters for all of the tall-grass simulations. The green color corresponds to more than 90% of solid fuel remaining, red to between 50% and 90% remaining, and brown to less than 50% remaining.

5. Discussion

The overall features of the simulations were quite similar for the local and nonlocal burning schemes. This similarity belies the fact that different fuel models were employed, one of which allowed for transport of the fuel before combustion while the other did not. Figure 5 shows an example of a 'flame' in the non-local fuel scheme, that is fuel combustion, and so heat release, away from the solid fuel.

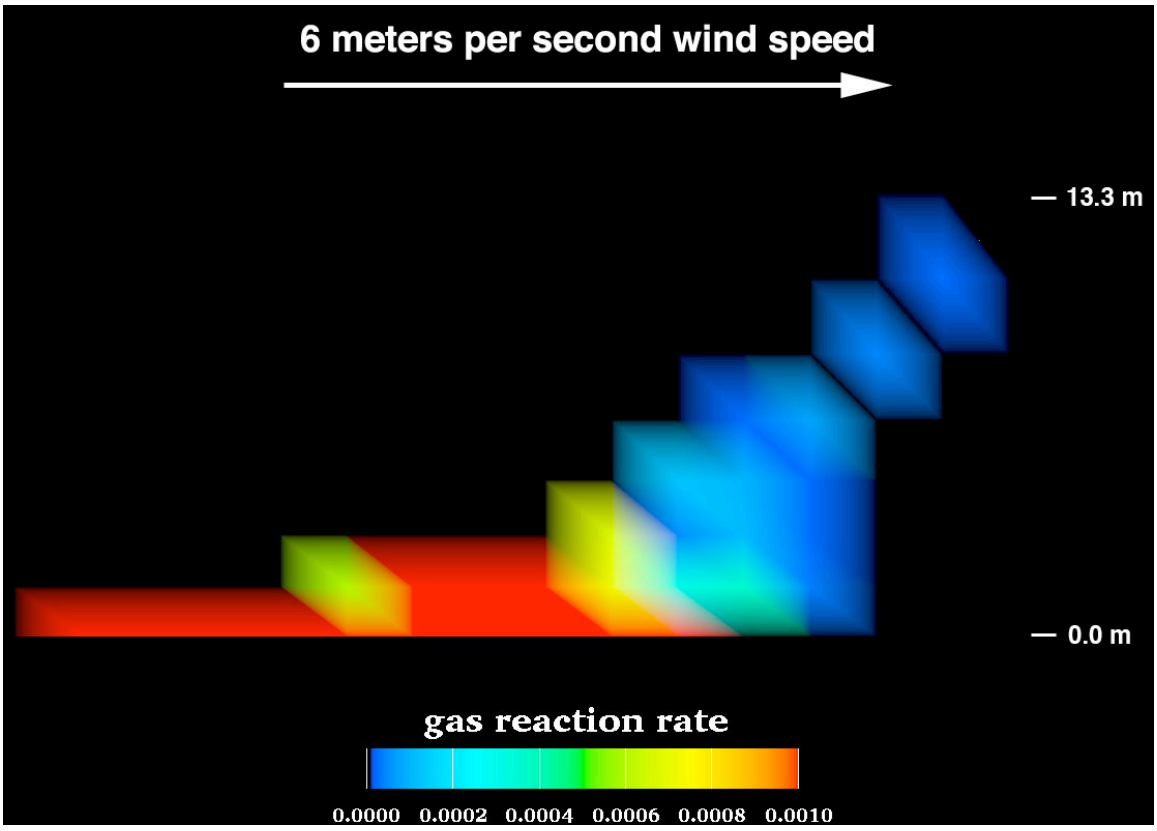

Figure 5. Cross-section of the gas reaction rate along the mid-line of the fire. The gas reaction rate is in units of kg/sec. This particular representation is from the u6 simulation along the leading edge of the fire after 60 seconds of simulated time have passed.

A significant fraction of the total reaction now occurs in locations that do not contain any solid fuel. There is only solid fuel in the bottom box in this simulation, corresponding to a lower boundary of 0.0 m and an upper boundary of 0.751 m, and with the local fuel model combustion could only take place there. The 'flame' depicted in Figure 5 extends up to a height of roughly 12 m (bottom of grid volume is at 10.7 m and the top at 13.3 m), though the rate of combustion is only on the order of 1% of the maximum rate. This represents a flame that might only occupy a fraction of the 10 m^3 volume grid location, for a fraction of the simulated time resolution of 0.02 seconds. Some tilt angle can be observed in the simulated flame but it is beyond the scope of this report to look for a specific relationship with inlet wind speed. The 'flame' certainly does tilt over more with increasing wind speed as would be expected qualitatively. In Figure 6 another 'flame' is presented, this time for an inlet wind speed of 3 m/sec. The reduced tilt angle is readily apparent, and the reduction in flame height as well. The flame in Figure 6 is roughly 5.6 m (bottom of grid volume at 4.7 m and the top at 6.5 m), of course this only represents the 4^{th} vertical grid point in our simulation. Figure 6 also depicts the relationship between the reactive gas reaction rate, the reactive gas concentration, and the gas temperature. Note that the gas reaction rate is directly proportional to heat release and indeed is the only source of heat in the simulation.

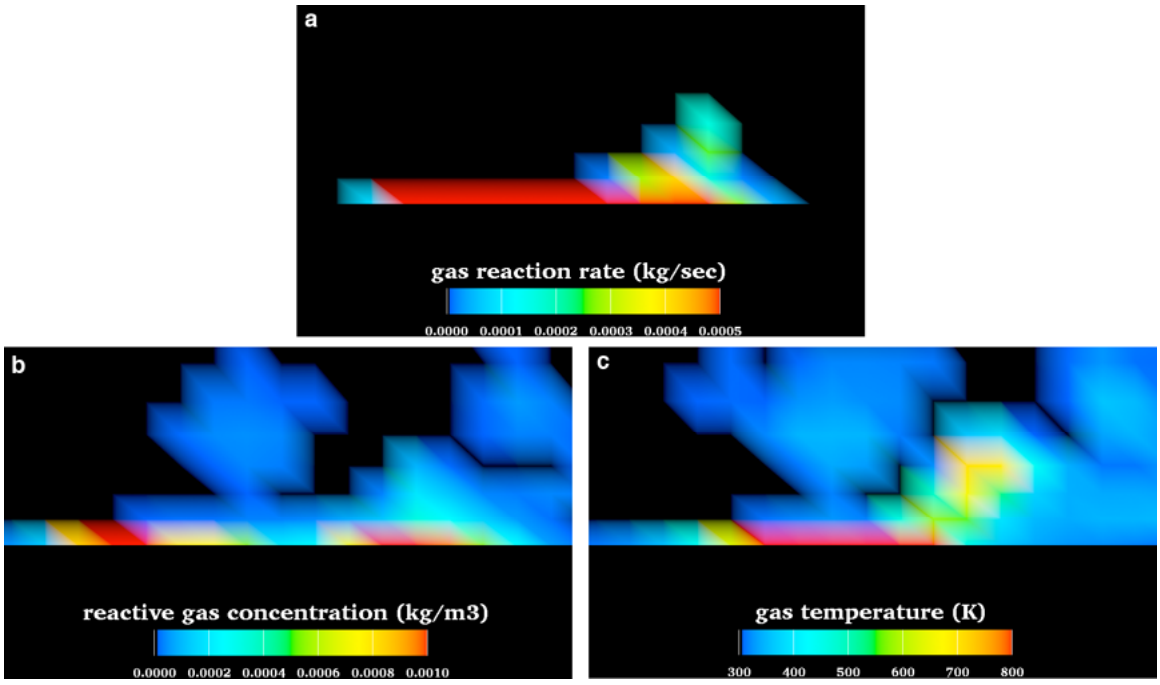

Figure 6. Cross-section of the gas parameters from the u3 simulation (inlet wind speed of 3 m/sec) along the mid-line of the fire near the leading edge of the fire after 60 seconds of simulated time have passed. Figure 5a depicts the gas reaction rate in units of kg/sec, figure 5b depicts the reactive gas concentration in units of kg/m^3, figure 5c depicts the gas temperature in units K.

Figure 6 shows that the gas reaction rate is limited by different factors in different locations. Though not evident in the figure the maximum gas reaction rate is located just behind the leading edge of the fire (value of about 0.04 kg/sec) where high reactive gas concentrations overlap with high gas temperatures. As one moves away from the leading edge of the fire the gas reaction rate drops off due to decreasing reactive gas concentrations even though gas temperatures are increasing; the gas reaction rate then increases with the gas concentration through a region of relatively constant gas temperatures, and finally drops off again with the gas temperature though gas concentrations are still increasing. Maximum gas temperatures occur in locations with relatively low reactive gas concentrations in part because the reactive gasses have a short residence time in those locations due to the high gas reaction rate.

5. Conclusion

A new nonlocal fuel model was implemented in HIGRAD/FIRETEC. It was found to give comparable results in a few simple test simulations utilizing idealized geometries. Computational resources were similar between the two fuel models. Additional work is needed to bring out the differences between the fuel models and to look at more extreme fire behaviors such as flash events, crowning, and fire 'whorls'.

5. Bibliography

Andrews PL (1986) BEHAVE: Fire Behavior Prediction and Fuel Modeling System-BURN Subsystem, Part 1. USDA Forest Service General Technical Report INT-194.

Clark TL, Jenkins MA, Coen J, Packham D (1996) 'A Coupled Atmosphere-Fire Model: Convective Feedback on Fire Line Dynamics'. *Journal of Applied Meteorology* **35**, 875- 901.

Coen JL, Clark TL (2000) 'Coupled Atmosphere-Fire Model Dynamics of a Fireline Crossing a Hill'. In 'Proceedings of the Third Symposium on Fire

and Forest Meteorology', January 2000, Long Beach, Ca.

Clark, T. L., J. Coen, et al. (2004). "Description of a coupled atmosphere-fire model." International Journal of Wildland Fire **13**(1): 49.

Dupey J-L, Larini M (2000) 'Fire spread through a porous forest fuel bed: A radiative and convective model including fire-induced flow effects'. *International Journal of Wildland Fire* **9**, 155-172.

Finney MA, (1998) FARSITE: Fire Area Simulator-Model Development and Evaluation. USDA Forest Service, Rocky Mountain Research Station Paper RMRS-RP-4. Ogden, UT.

Grishin AM (2001A) 'Heat and Mass Transfer and Modeling and Prediction of Environmental Catastrophes'. *Journal of Engineering Physics and Thermophysics* **74**, 895-903.

Grishin AM (2001B) 'Conjugate Problems of Heat and Mass Exchange and the Physicomathematical Theory of Forest Fires'. *Journal of Engineering Physics and Thermophysics* **74**, 904-911.

Hajaligol, M. R., J. B. Howard, et al. (1982). "PRODUCT COMPOSITIONS AND KINETICS FOR RAPID PYROLYSIS OF CELLULOSE." Ind Eng Chem Process Des Dev **21**(3): 457.

Linn RR (1997) 'Transport model for Prediction of Wildfire Behavior'. Los Alamos National Laboratory, Scientific Report LA13334-T.

Linn, R., J. Reisner, et al. (2002). "Studying wildfire behavior using FIRETEC." International Journal of Wildland Fire **11**(3-4): 233.

Linn, R., J. Winterkamp, et al. (2005). "Modeling interactions between fire and atmosphere in discrete element fuel beds." International Journal of Wildland Fire **14**(1): 37.

Linn, R. R. and P. Cunningham (2005). "Numerical simulations of grass fires using a coupled atmosphere-fire model: Basic fire behavior and dependence on wind speed." Journal of Geophysical Research-Atmospheres **110**(D13): D13107.

Nunn, T. R., J. B. Howard, et al. (1985). "PRODUCT COMPOSITIONS AND KINETICS IN THE RAPID PYROLYSIS OF MILLED WOOD LIGNIN." Ind Eng Chem Process Des Dev **24**(3): 844.

Nunn, T. R., J. B. Howard, et al. (1985). "PRODUCT COMPOSITIONS AND KINETICS IN THE RAPID PYROLYSIS OF SWEET GUM HARDWOOD." Ind Eng Chem Process Des Dev **24**(3): 836.

Reisner J, Wynne S, Margolin L, and Linn R (2000) 'Coupled-Atmospheric-Fire Modeling Employing the Method of Averages'. *Monthly Weather Review* **128**, 3683-3691.

Reisner J, Wyszogrodzki A, Mousseau V, Knoll D (2003) 'An efficient physics-based preconditioner for the fully implicit solution of small-scale thermally driven atmospheric flows'. *Journal of Computational Physics* **189**, 30-44.